CONF-770524--1

LOW-CYCLE FATIGUE AND CYCLIC DEFORMATION BEHAVIOR OF TYPE 16-8-2 WELD METAL AT ELEVATED TEMPERATURE

D. T. Raske

Prepared for

ASTM Symposium on Fatigue Testing of Weldments
Toronto, Canada
May 1977

U of C-AUA-USERDA

ARGONNE NATIONAL LABORATORY, ARGONNE, ILLINOIS

operated under contract W-31-109-Eng-38 for the
U. S. ENERGY RESEARCH AND DEVELOPMENT ADMINISTRATION

Low-cycle Fatigue and Cyclic Deformation Behavior of Type 16-8-2 Weld Metal at Elevated Temperature*

by

D. T. Raske

Materials Science Division
ARGONNE NATIONAL LABORATORY
Argonne, Illinois 60439

ABSTRACT: The low-cycle fatigue behavior of Type 16-8-2 stainless steel ASA weld metal at 593°C was investigated, and the results are compared with existing data for Type 316 stainless steel base metal. Tests were conducted under axial strain control and at a constant axial strain rate of 4×10^{-3} s^{-1} for continuous cyclic loadings as well as hold times at peak tensile strain. Uniform-gauge specimens were machined longitudinally from the surface and root areas of a 25.4-mm-thick welded plate and tested in the as-welded condition. Results indicate that the low-cycle fatigue resistance of this weld metal is somewhat better than that of the base metal for continuous-cycling conditions and significantly better for tension hold-time tests. This is attributed to the fine duplex delta ferrite-austenite microstructure in the weld metal. The initial monotonic tensile properties and the cyclic stress-strain behavior of this material were also determined. Because the cyclic changes in mechanical properties are strain-history dependent, a unique cyclic stress-strain curve does not exist for this material.

KEY WORDS: fatigue (materials), austenitic stainless steel weld metal, cyclic deformation, elevated-temperature testing, test equipment, cyclic straining, strains, stresses

---

*Work supported by the U.S. Energy Research and Development Administration.

Low-cycle Fatigue and Cyclic Deformation Behavior of Type 16-8-2 Weld Metal at Elevated Temperature*

by

D. T. Raske[1]

Type 16-8-2 (16% Cr-8% Ni-2% Mo) stainless steel weld metal has been used in the fabrication of elevated-temperature structural components since the 1950s [*1*].[2] More recently, this material is also undergoing tests to determine its suitability as a filler metal for Liquid Metal Fast Breeder Reactor (LMFBR) components fabricated from Type 316 stainless steel. As a result, Type 16-8-2 weld metal is well characterized in terms of its microstructural, creep-rupture, and monotonic tensile properties [*2-8*]. However, LMFBR components are operated under conditions where creep and fatigue damage can occur simultaneously, and, therefore the creep-fatigue properties, as well as the cyclic stress-strain properties, are of interest to designers.

The principal objective of the present study was to determine the creep-fatigue and cyclic stress-strain properties of Type 16-8-2 stainless steel weld metal deposited by the automatic submerged-arc (ASA) process and compare the results with existing data on Type 316 stainless steel tested at 593°C. Another goal was to continue development of the equipment and techniques necessary to perform creep-fatigue tests on weld metals.

This paper presents the results of continuous-cycling and tension hold-time (360 and 1.8×10^4 s) fatigue tests at 593°C on as-welded Type 16-8-2 stainless steel specimens that were machined longitudinally from the surface and root

---

*Work supported by the U.S. Energy Research and Development Administration.

[1]Mechanical Engineer, Materials Science Division, Argonne National Laboratory, Argonne, Ill. 60439.

[2]The italic numbers in brackets refer to the list of references appended to this paper.

areas of the weld. The initial monotonic tensile data and the cyclic stress-strain curves are also included.

Experimental Program

Type 316 Stainless Steel Base-line Data

Because variations between different heats and heat treatments can affect the continuous-cycling and creep-fatigue behavior of austenitic stainless steels [9-11], the comparison base-metal data was confined to that from one heat and heat treatment. The data used as the basis to compare the fatigue behavior of the weld metal were from Heat 65808 of Type 316 stainless steel in the solution-annealed condition [12,13] and are shown in Fig. 1.

Materials and Specimens

Type 316 stainless steel base-metal plates 25.4 mm thick were welded together by Babcock and Wilcox using the ASA process. The weld joint was a single V-groove with a 19-mm root opening and a 20° included angle. Approximately 20 passes were necessary to complete the weld. An analysis of the chemical composition of the Type 16-8-2 stainless steel weld metal is listed in Table 1. The microstructure of the weld metal consisted of ∿0.8 to 3.0 percent ferrite distributed in an austenite matrix [6]. Photomicrographs of both the weld and base metal (Heat 65808) are shown in Fig. 2.

Axially loaded uniform-gauge specimens in the as-welded condition were machined from the weld as shown in Fig. 3*a*. Specimens are designated LS (longitudinal surface) and LR (longitudinal root). Dimensions of the final specimen design are shown in Fig. 3*b*. This specimen design was used in lieu of the hourglass specimen traditionally employed in elevated-temperature tests because the weld metal is highly anisotropic and, consequently, a single diametral extensometer and strain computer cannot uniformly control the axial strain.

Initially, these specimens were designed without a taper over the 16.76-mm gauge section and were mechanically polished. However, room-temperature tests with strain gauges in the gauge section indicated the strain at the center of the straight gauge section was ∿15 percent lower than the strains controlled by the axial extensometer. Subsequent tests indicated that the taper shown in Fig. 3*b* would most nearly result in a uniform strain distribution over the gauge section. Mechanical polishing of this material to obtain the surface finish necessary to avoid premature failures proved to be excessively time consuming. Mechanically polished surfaces with a roughness $\gtrsim$0.2 μm resulted in failures that appeared to initiate at fine circumferential tool marks. Electropolishing with a solution of 60 percent phosphoric and 40 percent sulfuric acid for ∿120 s after an initial mechanical polish with 600-grit paper eliminated these problems, although the minimum roughness obtainable was only 0.4 μm.

Apparatus and Test Procedure

The tests were conducted in an MTS[3] closed-loop hydraulic test machine in air at 593°C with a constant axial strain rate $\dot{\varepsilon}$ of 4×10^{-3} s^{-1} using a triangular loading waveform. All but one test was started in the compressive direction, usually at a strain rate of 4×10^{-4} s^{-1}. This low strain rate was used because it resulted in an x-y plotter record that made calculation of the elastic modulus easier. The strain rate was increased after the first quarter cycle. This procedure was later abandoned because it was believed to contribute to specimen buckling, which will be discussed later. Failure was defined as complete separation of the specimen.

The majority of the specimens were tested in a loading fixture that had a three-post die set to provide accurate alignment during tests [*14*]. A number

---

[3]MTS Systems Corporation.

of experimental problems were encountered with this gripping arrangement. Unless the entire load train and specimen were in exact alignment, delayed buckling of the specimen occurred. Indeed, large bending strains could be induced in a specimen if the upper clamping plate bolts were tightened improperly. For these tests, two strain gauges 90° apart were used on each specimen in an area outside of the gauge section to facilitate mounting with a minimum of bending prior to testing. This procedure was found to be effective for elimination of the buckling problems experienced in earlier tests. At present, a self-aligning liquid metal grip, shown in Fig. 4, is used for testing. Using a precision-machined alignment specimen with strain gauges attached, the bending strains caused by this gripping arrangement were found to be ∿2 percent of the total strain range.

Specimen heating was accomplished by an induction coil operated at 455 kHz. The coil, shown in Fig. 4, was constructed to provide a uniform temperature distribution (±4°C) over the gauge section of the specimen. Power to the coil was provided by a Lepel high-frequency induction heater and was controlled by a thermocouple welded to the specimen. One additional thermocouple was placed on each side of the gauge section to monitor the temperature during tests. All thermocouples were located in the transition region 11.4 mm from the center of the gauge section to avoid initiation of cracks at the thermocouple welds. The temperature profile over the gauge section and the control thermocouple temperature were determined from 16 equally spaced thermocouples welded to a facsimile Type 316 stainless steel specimen. However, a later temperature profile on a Type 16-8-2 stainless steel specimen indicated that the control thermocouple on samples of this material must be operated at a higher temperature to obtain the desired 593°C over the gauge section. Consequently, several tests were conducted at a gauge-section temperature of 584°C. This, however,

did not appear to affect the results, as will be shown in the next section.

An axial extensometer with a gauge length of 11.68 mm was used to control longitudinal strain in the specimen. This extensometer, shown in Fig. 4, is supported by counterweights, and the extensometer tips are held in place on the specimen by friction. To date, no slippage has been observed nor have any failures initiated under the extensometer tips. Moreover, the locations of the crack-initiation sites around the circumference and along the gauge section of the specimens are random.

Results and Discussion

Continuous-cycling and Tension Hold-time Fatigue Tests

The results of this portion of the investigation are listed in Table 2. A comparison of these results and the strain-life curves from the Type 316 stainless steel base-line data is shown in Fig. 5. As observed in this figure, the resistance of the weld metal to the loadings is greater than that of the base metal. One significant exception to this observation is a continuous-cycling test at a strain range of 1 percent (specimen LS-2). This specimen was mechanically polished, and, although it is difficult to determine, the failure is believed to have initiated at a fine circumferential tool mark in the gauge section. As shown in Fig. 5, the fatigue lives for the specimens tested at 584 and 593°C are not significantly different, and in several cases specimens tested at 584°C had shorter fatigue lives than those tested at 593°C.

The results of the 360 and 1.0×10^4-s tension hold-time tests are particularly significant because the fatigue life for the weld metal is from three to seven times longer than that for the base metal when tested under the same conditions. This was unexpected since the creep-rupture properties of the weld metal are significantly poorer than the average properties for Type 316 stainless steel at 566 and 650°C [6]. Moreover, it has been statistically

established that heats of a similar austenitic stainless steel base metal, Type 304, with poor creep properties also tend to exhibit poorer than average creep-fatigue properties [10]. Thus, the correlation between creep and creep-fatigue behavior observed in base-metal samples is apparently not valid for weld metals.

One mechanism that may explain this difference is the mode of fatigue crack propagation in these materials. The results of crack-growth-rate studies on stainless steel weld- and base-metal samples indicate that the weld metal has significantly lower crack-growth rates than the base metal, particularly at 593°C [15-17]. This difference is attributed to the fine duplex delta ferrite-austenite microstructure in the weld metal which, with its many phase boundaries, inhibits the growth rate of cracks. Preliminary evidence that the fine microstructure of the weld metal is responsible for the observed differences in the fatigue lives of this material and the base metal was obtained from a specimen (LS-14) which was sectioned normal to the main crack and metallographically examined over the entire gauge section. All 88 cracks observed along both sides of the gauge section appeared to initiate at phase boundaries that intersected the surface of the specimen. Of this total, more than one third of the cracks stopped at either a phase-boundary triple point or a sharp break in an individual phase boundary. The propagation for the largest and several secondary cracks appeared to be almost entirely within the austenite matrix after a length of ~0.03 mm was attained within a phase boundary. In contract, the mode of crack propagation for the Type 316 stainless steel tested under the same conditions was reported to be intergranular [12].

Differences in fatigue lives attributed to nonmechanistic factors must also be considered. For example, they might be attributed to the fact that the weld-metal specimens were electropolished prior to testing, whereas the

base-metal specimens used for comparison were mechanically polished. However, the base-metal specimens were polished longitudinally to a 0.2-μm finish [18] and, as stated previously, the electropolished finish was only 0.4 μm. In addition, it has been shown that for the same degree of surface roughness, the difference between the low-cycle fatigue life for mechanical and electropolished specimens is insignificant [19].

Another potential source for the dissimilarity between these data may be the method of beginning the tests. All but one of the Type 316 stainless steel tests were begun with the first quarter cycle in tension. In contrast, all but one of the weld-metal tests were begun in the compressive direction. Although it had been reported that tests begun in tension would result in somewhat lower fatigue lives [14], recent studies [10] indicate that no statistically significant difference exists between tests begun in either manner.[4]

Finally, size effects also can be eliminated as a contributing factor to the observed differences in fatigue lives of the base and weld metal. A size effect based on the volume of the test specimen has been shown to exist, but the volume differences must be larger than those in the present study [20]. Moreover, the specimens with the largest volume (the uniform-gauge weld-metal specimens) would have the shortest fatigue lives, which was not observed.

Initial Monotonic Tensile Data and Cycle-dependent Changes in Mechanical Properties

The monotonic 0.2 percent offset yield strengths and the elastic modulus for the Type 16-8-2 stainless steel ASA weld metal as determined from the initial portion of the first-cycle hysteresis loops are listed in Table 3. These results indicate that the metal from the root of the weld has a higher yield strength than that from the weld surface. This is consistent with results obtained at Oak Ridge National Laboratory for this material at 565 and 649°C [6].

[4]Unpublished research by the author also supports this conclusion.

A prominent feature in the present data is the large scatter associated with the yield strength of the surface weld metal (more than twice that of the root weld metal). The scatter is probably due to differences in composition, structure, and local properties that result from the variety of thermal histories which occur in various locations of multipass weldments [2,4]. As expected, the elastic modulus exhibits relatively little scatter for these tests and is not statistically different for the surface and root weld metal.

The cyclic hardening and subsequent softening of the weld metal as a function of strain range and cycles are shown in Figs. 6 and 7. Note the widely differing values for the surface weld-metal stress range in Fig. 6. This is consistent with the large scatter in the monotonic yield-strength values discussed earlier. Beyond the last data point shown in these figures, the tensile stress amplitude drops to zero as failure of the specimen occurs.

The cyclic stress-strain curves shown in Fig. 8 were determined by two methods [27]. The lower curve (solid line) was obtained from the constant-amplitude continuous-cycling fatigue test data. A linear regression analysis was performed on the logarithms of the half-life stress $\Delta\sigma/2$ and plastic strain amplitudes from fatigue tests on both the surface and root weld metal. The results were of the form

$$\Delta\sigma/2 = K'(\Delta\varepsilon_p/2)^{n'} \tag{1}$$

where

K' = cyclic strength coefficient,

$\Delta\varepsilon_p$ = plastic strain range, and

n' = cyclic strain-hardening exponent.

Values of K', n', and the cyclic 0.2 percent offset yield strength are listed

in Table 3. The cyclic stress-strain curve was then calculated for the strain amplitude $\Delta\varepsilon/2$ using the relation [22]

$$\Delta\varepsilon/2 = \Delta\varepsilon_e/2 + \Delta\varepsilon_p/2 = \Delta\sigma/2E + (\Delta\sigma/2K')^{1/n'} \quad (2)$$

where

$\Delta\varepsilon_e$ = elastic strain range and

E = elastic modulus.

Initially, this exercise was performed for the surface and root weld metal individually. However, little difference exists between the calculated curves, particularly at low strains (<0.5 percent); thus, the data were combined to produce a single curve. At strains >0.5 percent (strain ranges >1.0 percent), the surface weld metal has slightly higher cyclic strength values, but the difference is not sufficiently large nor do adequate data exist to justify separate cyclic stress-strain curves.

The upper curve (broken line) in Fig. 8 was obtained from a monotonic tension test after cyclic straining on a single root weld-metal specimen. The preliminary straining consisted of blocks of gradually increasing and then decreasing strain amplitudes, i.e., incremental step tests interspersed with blocks of constant strain-range cycling. A total of ∿2100 cycles at strain ranges between 0.2 and 2.0 percent and a constant axial strain rate of 4×10^{-3} s^{-1} were imposed on the specimen prior to the monotonic tension test. Values of K' and n' for this stress-strain curve were determined by back-fitting incremental values of the logarithms of stress and plastic strain from the curve in Fig. 8 to the form of Eq 1 by a linear regression analysis. These values, as well as the 0.2 percent offset yield strength, are also listed in Table 3.

Normally the cyclic stress-strain curve for a given material can be generated by several methods, including those described above, which usually produce approximately the same results [27]. However, some materials, notably Type 304 stainless steel, respond differently to various loading histories and, thus, a unique cyclic-strain curve does not exist [9,23]. This results from the dependence of the cyclic hardening of the material on loading history. Since the material used in the present investigation is also an austenitic stainless steel, the different cyclic stress-strain curves shown in Fig. 8 were not unexpected. Although these curves provide widely different values of inelastic strain for a given stress, they both can be of value to designers. For example, if the anticipated loadings on a structural component were such that both large and small strain excursions would occur randomly, then the upper curve of Fig. 8 would be appropriate for characterization of these materials. If, however, the loadings were cyclically constant or increasing, the lower curve would be suitable for design purposes.

Conclusions

The results of the present investigation on Type 16-8-2 stainless steel ASA as-welded longitudinal specimens tested in air at 593°C and $\dot{\varepsilon} = 4 \times 10^{-3}$ s^{-1} suggest the following conclusions:

a. The resistance of this material to axial strain-controlled constant-amplitude continuous-cycling fatigue test loadings is greater than that of Type 316 stainless steel (Heat 65808) in the solution-annealed condition.

b. For 360 and 1.8×10^{4}-s tension hold-time fatigue tests, the cyclic life of this material is from three to seven times longer than that of Type 316 stainless steel. This is attributed to the fine duplex microstructure of the weld metal that inhibits the growth rate of cracks.

c. The correlation between resistance to static creep rupture and resistance to creep-fatigue failures previously observed in Types 304 and 316 stainless

steel base metals is not observed for this weld metal.

d. The monotonic 0.2 percent offset yield strength is higher in the root weld metal than in the surface weld metal. However, the elastic moduli for samples from both locations in the weld are identical.

e. This material is strain-history dependent, and, therefore, a unique cyclic stress-strain curve does not exist. Monotonic tension tests after cyclic straining result in a different stress-strain curve than obtained from companion fatigue tests at various completely reversed constant strain ranges.

Acknowledgments

The author is grateful for the help of J. C. Tezak, C. F. Peterson, and M. D. Gorman in the test program and data reduction. Special appreciation is due to W. F. Burke for his assistance in resolving the many experimental difficulties encountered in this investigation. Appreciation is also due to R. T. King of Oak Ridge National Laboratory for aid in procuring the material and for helpful discussions on the properties of weld metals. I also wish to thank D. R. Diercks and R. W. Weeks for their support and encouragement.

References

[1] Carpenter, O. R. and Wylie, R. D., *Metal Progress*, Vol. 70, No. 5, Nov. 1956, pp. 65-73.

[2] Ward, A. L., Irvin, J. E., Blackburn, L. D., Slaughter, G. M., Goodwin, G. M., and Cole, N. C., "Preparation, Characterization, and Testing of Austenitic Stainless Steel Weldments," HEDL-TME-71-118, Hanford Engineering Development Laboratory, Aug. 1971.

[3] Goodwin, G. M., Cole, N. C., and Slaughter, G. M., *Welding Journal*, Research Supplement, Vol. 51, No. 9, Oct. 1972, pp. 425s-429s.

[4] Ward, A. L., "Austenitic Stainless Steel Weld Materials--A Data Compilation and Review," HEDL-TME-74-25, Hanford Engineering Development Laboratory, May 1974.

[5] King, R. T., Cole, N. C., Berggren, R. G., and Goodwin, G. M., "Properties and Structure of 16-8-2 Stainless Steel Weld Metal," presented at the Second National Congress on Pressure Vessels & Piping, San Francisco, June 23-27, 1975, ASME Publication No. 75-PVP-45.

[6] King, R. T. and Edmonds, D. P., in "Mechanical Properties Test Data for Structural Materials Quarterly Progress Report for Period Ending April 30, 1976," ORNL-5150, Oak Ridge National Laboratory, pp. 135-146.

[7] Ward, A. L. and Blackburn, L. D., *Journal of Engineering Materials and Technology*, Transactions of the ASME, Series H, Vol. 98, No. 3, July 1976, pp. 213-220.

[8] Brinkman, C. R., Sikka, V. K., and King, R. T., "Mechanical Properties of LMFBR Primary Piping Materials," ORNL-5199, Oak Ridge National Laboratory, Nov. 1976.

[9] Brinkman, C. R. and Korth, G. E., "Heat-to-heat Variations in the Fatigue and Creep-fatigue Behavior of AISI Type 304 Stainless Steel at 593°C," *Journal of Nuclear Materials*, Vol. 48, 1973, pp. 293-306; also ANCR-1097, Aerojet Nuclear Company, May 1973.

[10] Diercks, D. R. and Raske, D. T., "Elevated-temperature Strain-controlled Fatigue Data on Type 304 Stainless Steel--A Compilation, Multiple Linear Regression Model, and Statistical Analysis," ANL-76-95, Argonne National Laboratory, Dec. 1976.

[11] Maiya, P. S. and Majumdar, S., in "Mechanical Properties Test Data for Structural Materials Quarterly Progress Report for Period Ending October 31, 1976," ORNL-5237, Oak Ridge National Laboratory, pp. 23-38.

[12] Brinkman, C. R., Korth, G. E., and Beeston, J. M., "Comparison of the Fatigue and Creep-Fatigue Properties of Unirradiated and Irradiated Type 304 and 316 Stainless Steel at 593°C (1100°F)," ANCR-1078, Aerojet Nuclear Company, Aug. 1972.

[13] Weeks, R. W., Diercks, D. R., and Cheng, C. F., "ANL Low-cycle Fatigue Studies—Program, Results, and Analysis," ANL-8009, Argonne National Laboratory, Nov. 1973.

[14] Slot, T., Stentz, R. H., and Berling, J. T., in *Manual on Low Cycle Fatigue Testing*, ASTM STP 465, American Society for Testing and Materials, 1969, pp. 100-128.

[15] James, L. A., *Welding Journal*, Research Supplement, Vol. 52, No. 4, April 1973, pp. 173s-179s.

[16] Shahinian, R., Smith, H. H., and Hawthrne, J. R., *Welding Journal*, Research Supplement, Vol. 51, No. 11, Nov. 1972, pp. 527s-532s.

[17] Raske, D. T. and Cheng, C. F., "Fatigue Crack Propagation in Types 304 and 308 Stainless Steel at Elevated Temperatures," submitted for publication in *Nuclear Technology*.

[18] Beeston, J. M. and Brinkman, C. R., in *Irradiation Effects on Structural Alloys for Nuclear Reactor Applications*, ASTM STP 484, American Society for Testing and Materials, 1970, pp. 419-450.

[19] Maiya, P. S. and Busch, D. E., *Metallurgical Transactions A*, Vol. 6A, Sept. 1975, pp. 1761-1766.

[20] Raske, D. T., "Section and Notch Size Effects in Fatigue," University of Illinois T&AM Report No. 360, Urbana, Ill., Aug. 1972.

[21] Landgraf, R. W., Morrow, JoDean, and Endo, T., *Journal of Materials*, JMLSA, Vol. 4, No. 1, March 1969, pp. 176-188.

[22] Raske, D. T. and Morrow, JoDean, in *Manual on Low Cycle Fatigue Testing*, ASTM STP 465, American Society for Testing and Materials, 1969, pp. 1-25.

[23] Jaske, C. E., Mindlin, H., and Perrin, J. S., in *Cyclic Stress-Strain Behavior Analysis, Experimentation, and Failure Prediction*, ASTM STP 519, American Society for Testing and Materials, 1973, pp. 13-27.

List of Figures

TABLE 1 -- *Chemical Composition of Type 16-8-2 Stainless Steel ASA Weld Metal (weight percent).*[a]

	C	Mn	P	S	Si	Cu	Ni	Cr	Mo	Ti	Nb	Ta	Co	N	B	V
Weld Center	0.047	1.48	0.026	0.012	0.89	0.09	10.03	14.85	1.76	0.010	0.030	0.03	0.09	0.028	<0.001	0.04
Final Pass	0.047	1.39	0.029	0.014	0.87	0.04	9.27	14.43	1.80	0.013	0.003	0.03	0.09	0.028	<0.001	0.04

[a] *From Ref 6.*

TABLE 2 — *Results*[a] *of Fatigue Tests on Type 16-8-2 Stainless Steel ASA Weld Metal As-Welded Longitudinal Specimens at 593°C and* $\dot{\varepsilon} = 4 \times 10^{-3}\ s^{-1}$.

Specimen Number	Location in Weld	Axial Strain Range, %		Tensile Hold Time, s	Stress at $N_f/2$, MPa		Fatigue Life		Remarks
		$\Delta\varepsilon_t$	$\Delta\varepsilon_p$		$\Delta\sigma$[b]	$\Delta\sigma_r$	N_f	t_f, ks	
LR-12	Root	2.03	1.43	0.0	302.6/299.7	...	367	3.70	...
LS-7	Surface	1.95	1.32	0.0	306.2/303.3	...	636	6.41	*c*
LS-13	Surface	1.50	0.95	0.0	262.5/267.6	...	1 407	11.04	*c,d*
LR-1	Root	1.50	1.00	0.0	255.6/250.7	...	1 576	11.88	...
LS-2	Surface	0.99	0.42	0.0	245.3/243.1	...	1 335	6.78	*c,d,e,* mechanically polished
LS-4	Surface	1.00	0.52	0.0	246.3/255.5	...	2 836	14.22	*d,e*
LR-5	Root	1.00	0.53	0.0	233.3/238.8	...	3 634	18.06	*e*
LS-12	Surface	0.51	0.15	0.0	187.4/191.0	...	27 906	69.78	*d,e*
LR-3	Root	0.50	0.12	0.0	185.7/170.9	...	31 155	77.58	*e*
LS-15	Surface	0.51	0.15	0.0	172.3/172.3	...	67 021[f]	168.84	*d,e*
LS-14	Surface	1.00	0.64	360	185.8/219.6	383.8	2 759[g]	1006.38	*d,e*
LR-7	Root	0.51	0.16	360	176.6/203.3	374.9	5 874	2128.98	...
LS-6	Surface	0.50	0.17	360	166.1/154.9	312.8	9 947	3605.80	...
LR-10	Root	2.03	1.54	1.8×10^4	237.7/246.5	421.1	>85[h]	~1536	...

[a] $\Delta\varepsilon_t$ = total strain range, $\Delta\varepsilon_p$ = plastic strain range, $\Delta\sigma$ = total stress range, $\Delta\sigma_r$ = relaxed stress range, N_f = cycles to failure, and t_f = time to failure.

[b] Peak tensile stress/peak compressive stress.

[c] Test started in tensile direction.

[d] Tested at 584°C.

[e] First quarter cycle at $\dot{\varepsilon} = 4 \times 10^{-4}\ s^{-1}$.

[f] Failed at tool mark in transition region; no visible cracks in gauge section.

[g] Machine shut down before failure; many large cracks in gauge section.

[h] Test stopped before failure as a result of programmer malfunction; several cracks in gauge section.

TABLE 3 -- *Type 16-8-2 Stainless Steel ASA Weld-metal Monotonic and Cyclic Tensile Data from Continuous-cycling Fatigue Tests on As-welded Longitudinal Specimens at 593°C and $\dot{\varepsilon} = 4 \times 10^{-3}$ and 4×10^{-4} s^{-1}.*

Location in Weld	Monotonic 0.2% Offset Yield Strength (σ_{ys}), MPa	Elastic Modulus (E) x 10^3, MPa	Cyclic Properties[a]		
			0.2% Offset Yield Strength (σ'_{ys}), MPa	Strength Coefficient (K'), MPa	Strain hardening Exponent (n')
Surface	214.1[b]	99.10[c]	231.9/270.3	688.0/475.3	0.175/0.094
Root	237.2[d]				

[a]Upper value from companion tests at constant strain ranges, lower value from monotonic tension tests after spectrum straining.

[b]Standard deviation = 40.90 MPa.

[c]Standard deviation = 5.75 MPa.

[d]Standard deviation = 18.88 MPa.

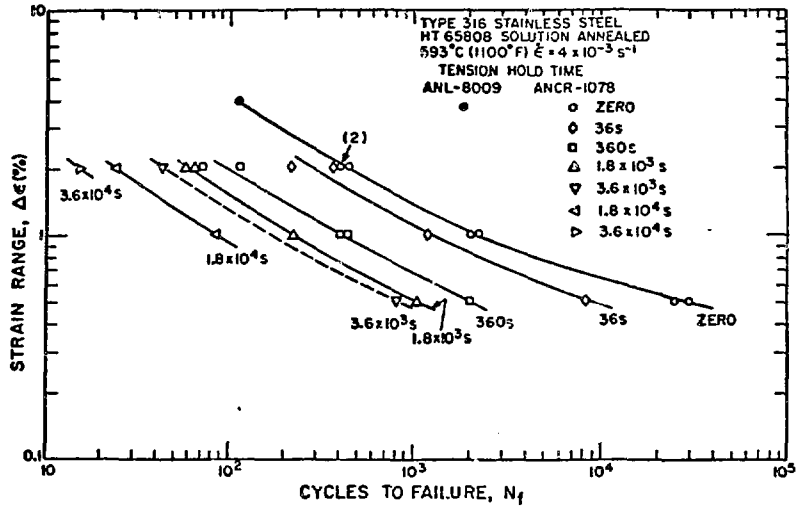

Fig. 1 -- Total Strain Range vs Cycles to Failure Showing Effect of Tension Hold Time on Fatigue Life for Type 316 Stainless Steel Base-line Data (Open Symbols from Ref 12, Solid Symbol from Ref 13. MSD-63754.

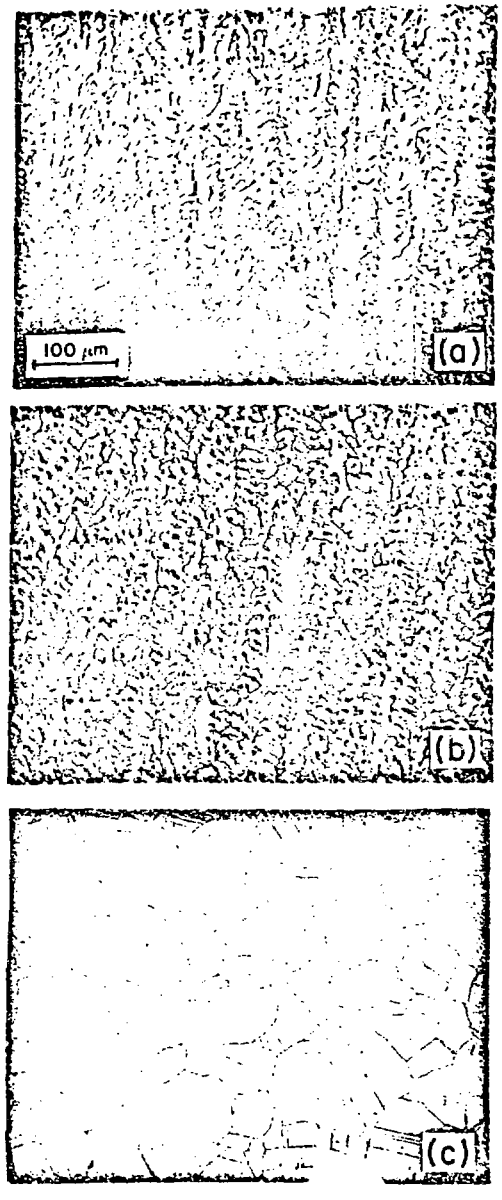

(*a*) Root weld metal.

(*b*) Surface weld metal.

(*a*) Base metal.

Fig. 2 -- Microstructures of Type 16-8-2 Stainless Steel ASA Weld Metal and Type 316 Stainless Steel Base Metal. Oxalic acid. MSD-63953.

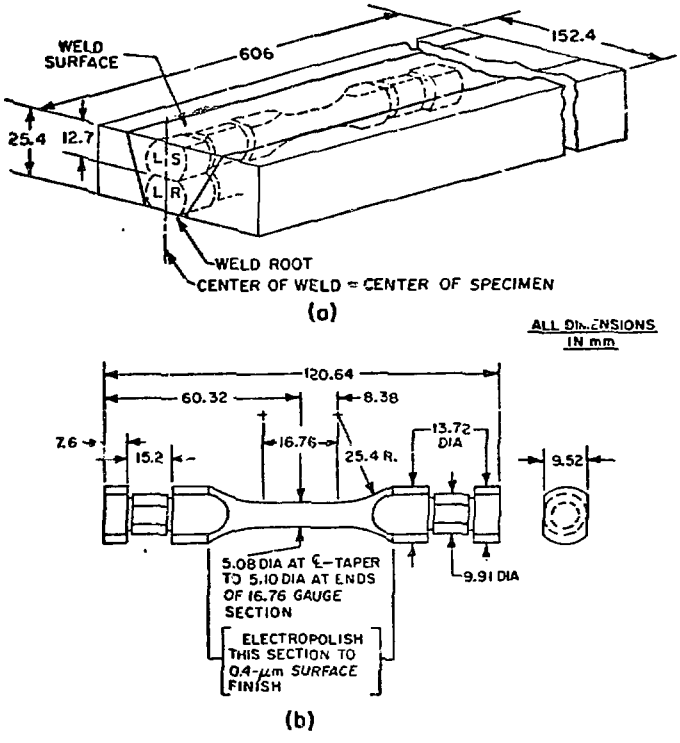

Fig. 3 -- Type 16-8-2 Stainless Steel ASA Weld-metal Test Specimens. MSD-63753.

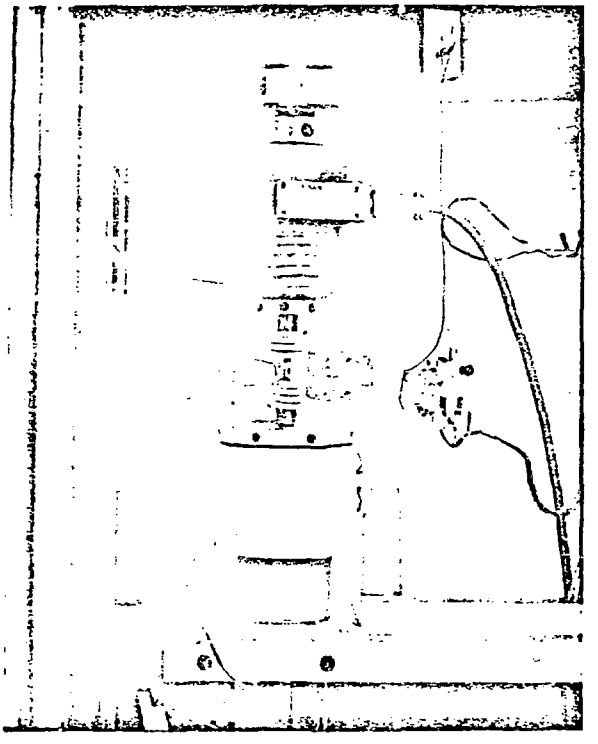

Fig. 4 -- Photograph of Liquid Metal Grip Showing a Specimen in Place Surrounded by Induction Heating Coil and the Axial Extensometer Attached. MSD-63954.

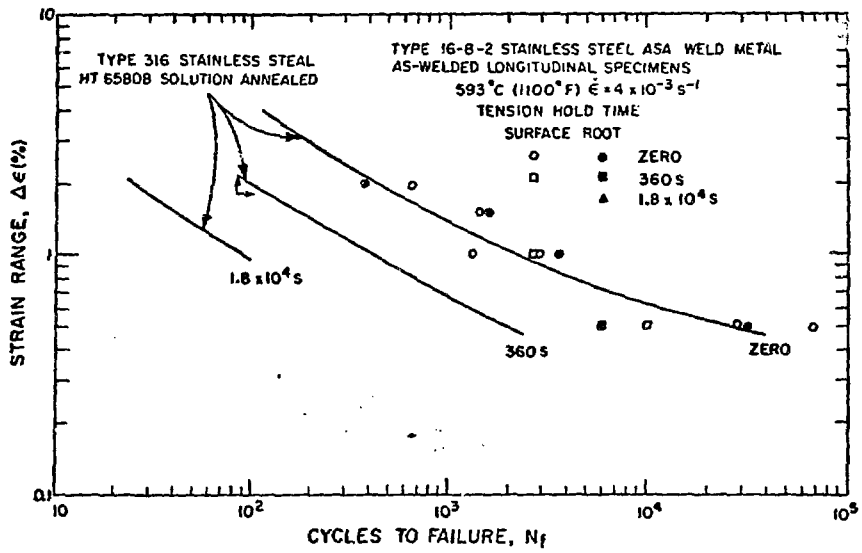

Fig. 5 — Total Strain Range vs Cycles to Failure for Type 16-8-2 Stainless Steel ASA Weld Metal Compared with Type 316 Stainless Steel Baseline Data. MSD-63949.

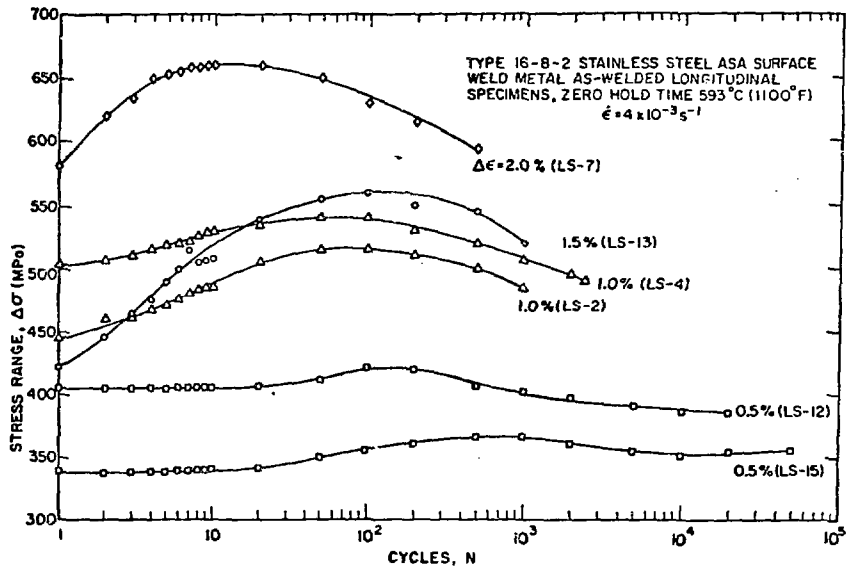

Fig. 6 -- Changes in Stress Range during Reversed Strain Cycling for Surface Weld Metal (Specimen Numbers in Parentheses). MSD-63951.

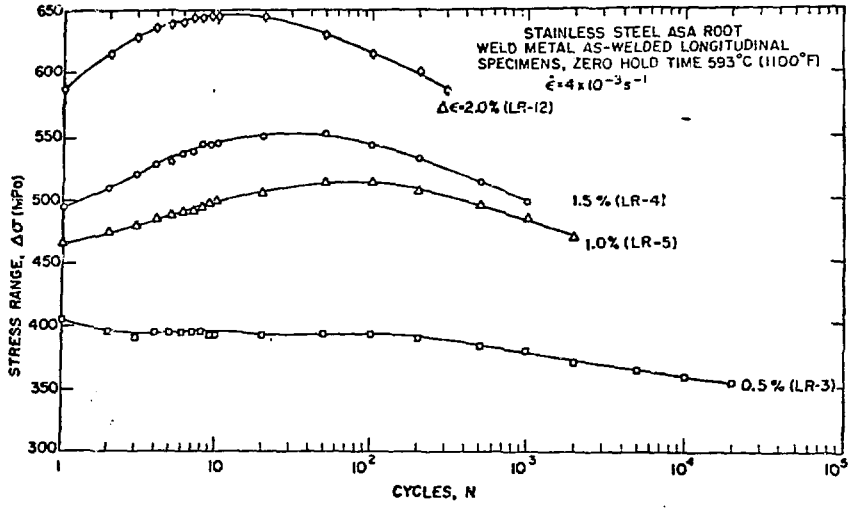

Fig. 7 -- Changes in Stress Range during Reversed Strain Cycling for Root Weld Metal (Specimen Numbers in Parentheses). MSD-63950.

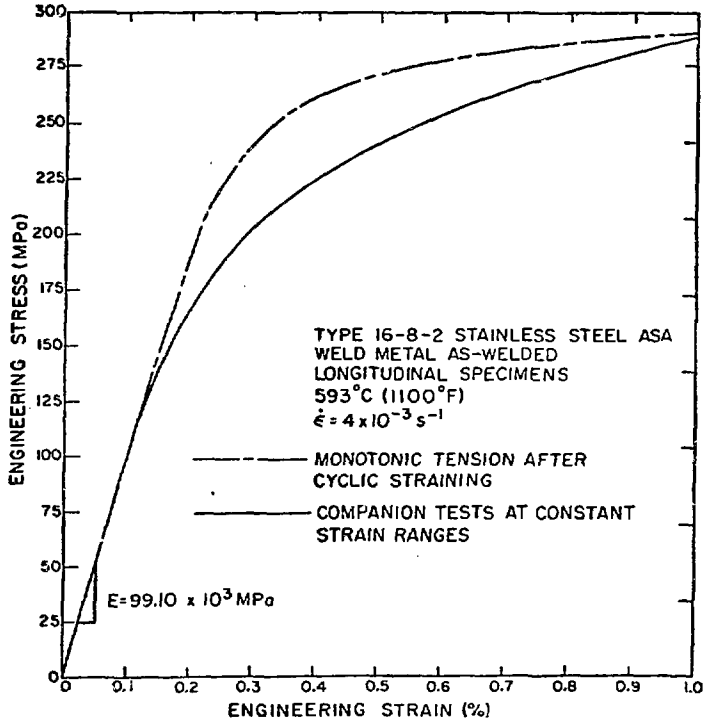

Fig. 8 -- Cyclic Stress-Strain Curves from Constant-amplitude Continuous-cycling Fatigue Tests and Monotonic Tension Test after Cyclic Straining. MSD-63952.